Challenges and Issues of Modern Science
2026, Vol. 5, No. 1, ID 341
ISSN: 3083-5704
URL: https://cims.fti.dp.ua/j/article/view/341
DOI: https://doi.org/10.15421/cims.5.341

UDC 544.723:628.336

Multi-Feedstock Biochar from Lignocellulosic Biomass: Synthesis and Dye Adsorption Performance

Deshraj Singh Thakur, Santosh Narayan Chadar

Purpose. This study developed a multi-feedstock biochar (MFB) from lignocellulosic biomass — teak wood, coconut shell, sugarcane bagasse, maize straw, and peanut shell — to enhance methylene blue adsorption through cooperative interactions between various biomass feedstocks. **Design / Method / Approach.** MFB was synthesized by controlled pyrolysis at 500–700 °C under inert atmosphere and characterized using BET, SEM, FTIR, XRD, zeta potential, and DLS analyses. Adsorption performance toward methylene blue was assessed through batch experiments and modeled using kinetic, isotherm, and thermodynamic approaches. **Findings.** MFB exhibited a BET surface area of 76.6 $m^2 g^{-1}$, a hierarchical pore structure, and diverse surface functional groups, collectively improving dye adsorption efficacy. Under optimized conditions, more than 95% of methylene blue was removed within 90 minutes. Adsorption fitted the Langmuir isotherm and pseudo-second-order kinetic models, confirming monolayer chemisorption; thermodynamic analysis indicated a spontaneous and endothermic process driven by pore diffusion, π–π interactions, hydrogen bonding, and electrostatic attraction. **Theoretical Implications.** The results demonstrate that combining several biomass feedstocks produces synergistic physicochemical properties difficult to achieve with single-feedstock biochar, advancing the mechanistic understanding of multi-component biochar adsorbents. **Practical Implications.** The use of widely available biomass waste makes MFB a scalable, affordable, and sustainable solution for dye-contaminated wastewater treatment. **Originality / Value.** Unlike conventional single-feedstock approaches, this study systematically examines how feedstock integration governs pore structure, surface heterogeneity, and adsorption mechanisms, demonstrating that synergistic biomass combination enhances adsorption performance beyond simple feedstock substitution. **Research Limitations / Future Research.** The study is limited to laboratory-scale experiments with synthetic dye solutions; future work should address regeneration performance, long-term stability, real wastewater treatment, and pilot-scale validation. **Article Type.** Empirical Research Paper.

Keywords:

methylene blue, adsorption kinetics, biomass valorization, porous carbon materials, surface functional groups, wastewater treatment

Мета. У цьому дослідженні отримано мультисировинне біовугілля (МСБ) з лігноцелюлозної біомаси — деревини тика, кокосової шкаралупи, багасу цукрової тростини, кукурудзяної соломи та лушпиння арахісу — для підвищення ефективності адсорбції метиленового синього через синергетичну взаємодію різних видів сировини. **Дизайн / Метод / Підхід.** МСБ синтезовано контрольованим піролізом при 500–700 °C в інертній атмосфері та охарактеризовано методами BET, SEM, FTIR, XRD, дзета-потенціалу і DLS; адсорбційні характеристики щодо метиленового синього оцінено в серійних експериментах із застосуванням кінетичних, ізотермічних і термодинамічних моделей. **Результати.** МСБ має питому поверхню 76,6 $м^2 г^{-1}$, ієрархічну пористу структуру та різноманітні поверхневі функціональні групи, що в сукупності підвищують ефективність адсорбції барвника. За оптимальних умов видалено понад 95% метиленового синього за 90 хвилин; адсорбція відповідає ізотермі Ленгмюра та моделі псевдодругого порядку, підтверджуючи моношарову хемосорбцію, а термодинамічний аналіз свідчить про спонтанний ендотермічний процес, зумовлений поровою дифузією, π–π-взаємодіями, водневими зв'язками та електростатичним притяганням. **Теоретичне значення.** Отримані результати демонструють, що інтеграція кількох видів біомаси забезпечує синергетичні фізико-хімічні властивості, недосяжні для однокомпонентного біовугілля, поглиблюючи механістичне розуміння багатокомпонентних адсорбційних систем. **Практичне значення.** Використання доступних відходів біомаси робить МСБ масштабованим, економічно доступним і екологічно сталим рішенням для очищення стічних вод від барвників. **Оригінальність / Цінність.** На відміну від традиційних однокомпонентних підходів, дослідження системно аналізує вплив інтеграції сировини на пористу структуру, поверхневу гетерогенність і механізми адсорбції, демонструючи переваги синергетичного поєднання біомаси над простою заміною сировини. **Обмеження / Майбутні дослідження.** Роботу виконано в лабораторному масштабі із синтетичними розчинами барвників; подальші дослідження мають охоплювати регенерацію адсорбенту, довготривалу стабільність, очищення реальних стічних вод і пілотну валідацію. **Тип статті.** Емпірична стаття.

Ключові слова:

метиленовий синій, кінетика адсорбції, валоризація біомаси, пористі вуглецеві матеріали, поверхневі функціональні групи, очищення стічних вод

Contributor Details:

Deshraj Singh Thakur, Postgraduate Student, Government Autonomous Girls Postgraduate College of Excellence: Sagar, Madhya Pradesh, IN, deshrajthakur117@gmail.com
Santosh Narayan Chadar, Assistant Professor, Government Autonomous Girls Postgraduate College of Excellence: Sagar, Madhya Pradesh, IN, dr.santoshnarayan@gmail.com

Received: 2026-04-24 *Revised: 2026-05-16* *Accepted: 2026-05-18* *Published: 2026-05-26*

The durability, toxicity, and complex chemical structure of synthetic dyes have made the discharge of dye-containing effluents from the textile, paper, leather, printing, and dye-manufacturing sectors a major environmental issue. Because of their synthetic origin and aromatic chemical structures, most synthetic dyes are resistant to biodegradation and remain stable in natural environments (Forgacs et al., 2004). According to Chien and Ganesan (2024), dyes have a negative impact on aquatic organisms and human health, even at low concentrations; they also inhibit photosynthesis and reduce light penetration in aquatic systems. Additionally, dye-contaminated wastewater raises chemical and biological oxygen demands (BOD and COD), disrupting microbial activity and ecological equilibrium in receiving water bodies (Chien & Ganesan, 2024). Because azo dyes can degrade into toxic, mutagenic, and carcinogenic aromatic amines, they pose substantial environmental and health risks (Josephy & Allen-Vercoe, 2023). Furthermore, interactions of dye molecules with soil minerals and natural organic matter may promote adsorption and environmental persistence of dye-derived compounds. These environmental risks highlight the need for effective, sustainable, and economically feasible wastewater treatment technologies.

Because of its ease of use, high removal effectiveness, low energy consumption, and adaptability to various wastewater treatment conditions, adsorption is widely acknowledged as an efficient approach among the existing treatment methods (Crini & Lichtfouse, 2018). Because of its large surface area, tunable surface chemistry, porous carbonaceous structure, and oxygen-containing functional groups that promote pollutant adsorption, biochar has garnered significant attention as a sustainable adsorbent in recent years (Ahmad et al., 2012; Inyang & Dickenson, 2015; Mohan et al., 2014). The mineral concentration, pore distribution, surface functionality, pyrolysis conditions, and biomass composition all have a significant impact on the adsorption performance of biochar. Adsorption mechanisms such as electrostatic attraction, hydrogen bonding, π–π interactions, pore filling, ion exchange, and surface complexation are all influenced by these characteristics (Ahmad et al., 2014).

The significance of engineered biochar systems for environmental remediation has been highlighted by recent studies (Tan et al., 2016; Wang & Wang, 2019; Lodhi et al., 2024). By enhancing pore accessibility and the density of active functional groups, surface modification and structural engineering improve adsorption effectiveness (Tan et al., 2016). Similarly, due to their increased surface area and improved surface reactivity, activated and nano-engineered biochar composites exhibit better adsorption (Inyang & Dickenson, 2015). Prior research has also demonstrated that the choice of feedstock has a significant impact on the physicochemical properties and adsorption performance of biochar. Woody biomass-derived biochars typically have higher aromaticity, fixed carbon content, and structural stability (Sun et al., 2013), while agricultural biomass-derived biochars have higher ash content and oxygen-containing functional groups that promote polar contaminant adsorption (Chen et al., 2014).

Despite these developments, most published research has focused on single-feedstock biochars made from woody biomass or agricultural residues. Even though this research offers valuable insights into feedstock-dependent adsorption behavior, many studies only vary the precursor biomass while using similar synthesis protocols, characterization techniques, and adsorption models. Consequently, it remains challenging to determine whether improvements in adsorption performance derive from actual structural and chemical enhancement or merely from biomass substitution.

According to recent advances in biochar engineering, combining multiple biomass feedstocks can offer a more promising approach to developing sophisticated adsorbents with improved physicochemical properties and adsorption performance (Li et al., 2017; Aziz et al., 2024). While woody biomass enhances carbon stability and structural integrity during pyrolysis, agricultural residues promote pore formation and surface functionalization. Pore architecture, surface heterogeneity, adsorption site distribution, adsorption kinetics, and pollutant interaction mechanisms can therefore be modified by combining multiple biomass types in ways that are not possible with single-feedstock systems. Nevertheless, systematic studies examining the adsorption behavior and mechanistic benefits of multi-feedstock biochar systems remain scarce.

The need to transition from traditional single-feedstock biochar systems to multifunctional and synergistically designed carbon materials for sustainable environmental remediation has been further highlighted by recent review studies (Yaashikaa et al., 2020). However, only a few studies have thoroughly investigated the effects of feedstock integration on equilibrium behavior, surface chemistry, adsorption mechanisms, and dye removal efficiency.

This work develops and evaluates a multi-feedstock biochar (MFB) from woody and agricultural lignocellulosic biomass for efficient dye adsorption from aqueous solutions. **The objectives of this study** are to: (i) synthesize MFB and apply structural and surface analytical techniques to characterize its physicochemical properties; (ii) evaluate its adsorption performance toward methylene blue under various operating conditions; and (iii) investigate the adsorption mechanism using kinetic, isotherm, thermodynamic, and surface interaction analyses.

Materials and Methods

Materials and Reagents

Teak wood chips and coconut shells were acquired from local biomass processing facilities, while sugarcane bagasse, maize straw, and peanut shells were gathered from nearby agricultural fields. These feedstocks were selected to create a multi-feedstock biochar with complementary physicochemical properties. Agricultural residues were included for their high cellulose and hemicellulose content, which promotes pore formation and the development of oxygen-containing functional groups during pyrolysis. Woody biomass was included for its higher lignin content, which enhances the biochar matrix's aromaticity, fixed carbon content, and structural stability (Weber & Quicker, 2018; Yang et al., 2024).

Methylene blue (MB, analytical grade, ⩾99% purity) was purchased from Sigma-Aldrich. Sodium hydroxide (NaOH, 0.1 M, analytical grade) and hydrochloric acid (HCl, 0.1 M, analytical grade), used for pH adjustment, were supplied by Merck. Deionized water was used throughout the experiments.

Feedstock Selection and Preparation

The collected biomass materials were thoroughly washed with deionized water to remove dust, dirt, and other surface impurities. After cleaning, the feedstocks were oven-dried at 105 °C for 24 hours until constant weight was achieved. The dried materials were then ground in a laboratory grinder and sieved to a particle size below 100 mesh. Equal amounts of agricultural and woody biomass feedstocks were mixed to prepare the precursor material for multi-feedstock biochar synthesis. The mixed feedstocks were stored in sealed polyethylene containers prior to pyrolysis experiments.

Biochar Synthesis

Multi-feedstock biochar (MFB) was produced by controlled pyrolysis under oxygen-limited conditions using a muffle furnace (NISIF India MR 85(1.5)) and a stainless-steel tube reactor (SS310 grade). To ensure an inert atmosphere and prevent oxidative degradation during thermal treatment, high-purity nitrogen gas (99.99%) was continuously supplied at a flow rate of 100 mL min^{-1} throughout the pyrolysis process.

Approximately 20 g of the prepared biomass mixture was loaded into the reactor and heated at a constant rate of 10 °C min^{-1} from ambient temperature to 500–700 °C. This temperature range was selected because intermediate-to-high pyrolysis temperatures significantly influence aromatic carbon development, pore formation, mineral transformation, and surface functionalization of biochar materials (Thakur & Chadar, 2025a). Isothermal conditions were maintained for four hours after reaching the target temperature to ensure complete carbonization and stabilization of the biochar matrix. Following pyrolysis, the furnace was allowed to cool naturally to room temperature under continuous nitrogen flow to prevent oxidation of the product. The biochar was then collected, crushed into a fine powder, and stored in airtight glass containers for further analysis and adsorption experiments.

The multi-feedstock approach was employed to examine whether combining cellulose-rich agricultural residues with lignin-rich woody biomass could enhance pore accessibility, surface heterogeneity, and the density of adsorption-active functional groups compared to traditional single-feedstock biochar systems.

Characterization Techniques

The surface, morphological, and structural properties of the synthesized biochar were evaluated using a suite of analytical techniques to establish their relationship to adsorption performance.

Brunauer–Emmett–Teller (BET) analysis was performed using a Quantachrome Instruments NOVA 2200e/4200e surface area analyzer to determine specific surface area, pore volume, and pore size distribution, providing key insights into porosity and adsorption-active surface area.

Surface morphology and pore structure were investigated by scanning electron microscopy (SEM; Nova NanoSEM 450, FEI Company) (Goldstein et al., 2018), enabling observation of surface roughness, pore formation, and structural changes induced by pyrolysis.

Fourier-transform infrared spectroscopy (FTIR; ALPHA II spectrometer, Bruker Optics) was performed over the wavenumber range of 4000–400 cm^{-1} to identify surface functional groups — including hydroxyl, carboxyl, and aromatic groups — involved in adsorbate–adsorbent interactions.

X-ray diffraction (XRD; D8 ADVANCE diffractometer, Bruker AXS) with Cu-Kα radiation (λ = 1.5406 Å) was used to examine the crystalline structure and mineral phase composition, assessing structural ordering and inorganic mineral phases within the biochar matrix (Cullity & Stock, 2001).

Surface charge characteristics and particle size distribution were measured using a Zetasizer Nano ZS analyzer (Malvern Panalytical), applying zeta potential and dynamic light scattering (DLS) analyses to evaluate colloidal stability, particle dispersion behavior, and surface charge interactions in relation to dye adsorption.

Batch Adsorption Experiments

The adsorption performance of the synthesized multi-feedstock biochar toward methylene blue removal was assessed through batch experiments conducted in 250 mL Erlenmeyer flasks containing a known mass of adsorbent and a fixed volume of dye solution. Suspensions were agitated at 150 rpm using an orbital shaker (Remi CIS-24 Plus, India) until equilibrium was achieved. All experiments were conducted in triplicate under controlled laboratory conditions, and results are reported as mean ± standard deviation.

The effects of operational parameters on adsorption performance were systematically examined. Initial dye concentration was varied between 10 and 200 mg L^{-1} to assess equilibrium behavior and adsorption capacity. Solution pH was adjusted between 2 and 10 using 0.1 M HCl or 0.1 M NaOH to investigate the influence of surface charge interactions and dye ionization. Contact time was varied between 0 and 180 minutes to determine equilibrium time and adsorption kinetics. Adsorbent dosage was varied from 0.1 to 1.0 g L^{-1} to evaluate the relationship between removal efficiency and adsorption site availability. Thermodynamic experiments were carried out at 298–318 K to assess the energetic feasibility and temperature dependence of the adsorption process.

Following adsorption, suspensions were vacuum-filtered through mixed cellulose ester membrane filters (Millipore, 0.45 μm pore size) to remove suspended biochar particles prior to spectrophotometric measurement. Residual methylene blue concentration was determined at the maximum absorption wavelength of 664 nm using a UV–visible spectrophotometer (Shimadzu UV–1800, Japan).

Adsorption capacity and dye removal efficiency were calculated using equations (1) and (2), respectively:

$$q_e = \frac{(C_0 - C_e)V}{m}, \quad (1)$$

$$\text{Removal } (\%) = \frac{C_0 - C_e}{C_0} \times 100, \quad (2)$$

where C_0 and C_e represent the initial and equilibrium dye concentrations (mg L^{-1}), respectively, V is the solution volume (L), and m is the mass of adsorbent (g).

Adsorption Modelling and Statistical Analysis

Adsorption kinetics, equilibrium behavior, and thermodynamic feasibility were evaluated using established adsorption models selected based on the expected adsorption mechanisms and surface interaction characteristics of biochar-based adsorbents.

The pseudo-first-order model was applied to analyze physisorption-controlled adsorption, the pseudo-second-order model to evaluate chemisorption involving electron sharing or exchange between adsorbent and adsorbate molecules, and the intraparticle diffusion model to examine diffusion-controlled mass transfer and pore diffusion contributions. Equilibrium adsorption data were fitted to the Langmuir, Freundlich, and Temkin isotherm models (Foo & Hameed, 2010). The Langmuir model assessed monolayer adsorption on homogeneous sites (Langmuir, 1918), the Freundlich model described heterogeneous surface adsorption and multilayer interactions, and the Temkin model characterized adsorbate–adsorbent interactions and adsorption heat distribution across the biochar surface.

The spontaneity and energetic nature of the adsorption process were assessed using thermodynamic parameters — Gibbs free energy (ΔG°), enthalpy change (ΔH°), and entropy change (ΔS°).

Model fitting was evaluated using the correlation coefficient (R^2), root mean square error (RMSE), and chi-square error function (χ^2) to identify the best-fit model and support mechanistic interpretation of adsorption behavior.

All experimental data were analyzed using OriginPro 2024. Statistical analyses were performed on triplicate measurements, and results are reported as mean ± standard deviation to ensure reproducibility and methodological transparency.

Results and Discussion

Elemental Composition Analysis (EDX)

Energy-dispersive X-ray spectroscopy (EDX) in conjunction with scanning electron microscopy (SEM; Nova NanoSEM 450, FEI Company) was used to examine the elemental composition and surface elemental distribution of the synthesized MFB (Goldstein et al., 2018). The EDX spectrum displayed in Figure 1 confirms that the synthesized adsorbent was primarily carbonaceous, directly addressing Objective (i) concerning the physicochemical characterization of the material.

A prominent peak at approximately 0.27 keV corresponding to carbon (C Kα) confirmed successful thermal carbonization of the lignocellulosic biomass during pyrolysis. The high carbon intensity indicates the formation of a persistent aromatic carbon framework favorable for adsorption applications, as aromatic carbon domains promote π–π interactions with methylene blue molecules. A distinct peak at approximately 0.52 keV corresponding to oxygen (O Kα) confirmed the presence of oxygen-containing surface functional groups formed during pyrolysis and partial surface oxidation; these oxygenated groups contribute to adsorption through surface complexation, electrostatic attraction, and hydrogen bonding. A smaller peak near 3.69 keV attributed to calcium (Ca Kα) indicated the presence of residual inorganic mineral components inherited from the biomass precursors.

The quantitative elemental composition is summarized in Table 1. Carbon was the dominant element at 90.03 wt.% (93.31 at.%), followed by oxygen at 7.68 wt.% (5.98 at.%) and calcium at 2.28 wt.% (0.71 at.%). The high carbon content confirmed the formation of a well-carbonized structure with high aromaticity and structural stability. The oxygen content indicated that the synthesized biochar retained sufficient oxygen-containing functional groups for adsorption-active surface interactions. The low calcium level was attributed to naturally occurring ash-forming minerals retained during thermal decomposition of the biomass feedstocks.

The synthesized MFB showed greater elemental variability than previously reported single-feedstock biochars, attributed to the combined input of woody and agricultural biomass sources. This compositional diversity produced chemically heterogeneous adsorption-active sites with higher affinity for dye molecules, supporting the synergistic effect of feedstock integration proposed in the Introduction. The relatively low uncertainty in oxygen and calcium measurements indicated uniform elemental distribution across the examined surface region, while the slightly higher deviation in carbon content reflected the heterogeneous microstructure typical of multi-feedstock-derived carbon materials. Overall, EDX analysis confirmed that the synthesized MFB features a carbon-rich structure with oxygen-containing functional groups and trace mineral components, supporting Objective (i) on the physicochemical characterization of the developed adsorbent for dye removal.

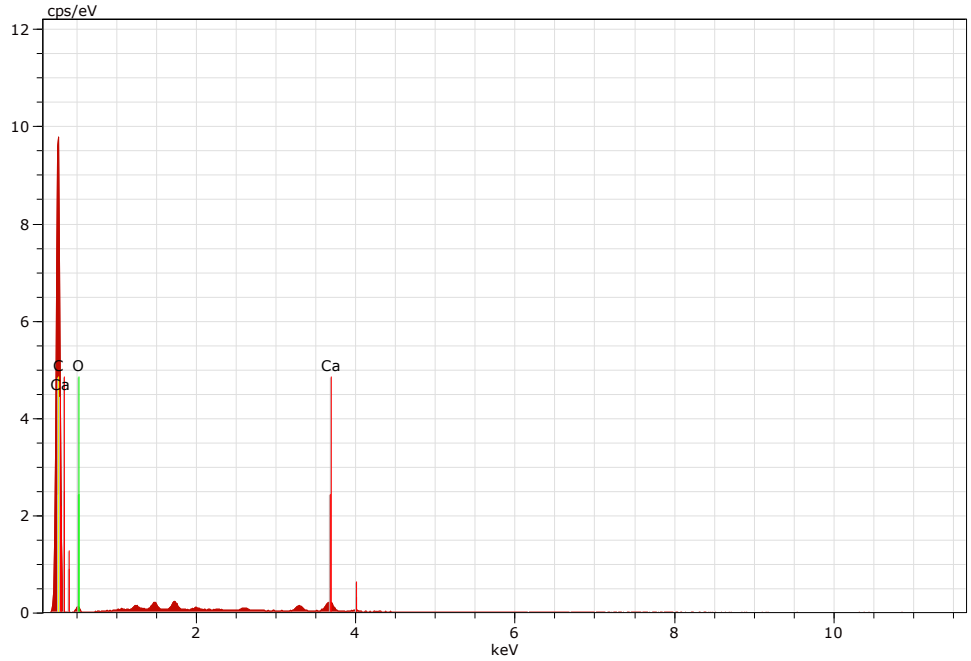

Figure 1 – The EDX spectrum has a dominant C with modest O and Ca (Source: Authors)

Table 1 – Elemental composition of MFB determined by EDX analysis (Source: Authors)

Element	Atomic Number	Series	Weight % (wt.%)	Normalized wt.%	Atomic % (at.%)	Error (± wt.%)
C	6	K-series	90.03	90.03	93.31	10.24
O	8	K-series	7.68	7.68	5.98	1.68
Ca	20	K-series	2.28	2.28	0.71	0.10
Total	—	—	100.00	100.00	100.00	—

Surface Morphology Evolution of the Material (SEM)

Scanning electron microscopy (SEM; Nova NanoSEM 450, FEI Company) was used to analyze the surface morphology and structural evolution of the synthesized MFB. Figures 2a–2d present representative micrographs, addressing Objective (i) by assessing pore development, surface roughness, and structural heterogeneity resulting from multi-feedstock pyrolysis.

Figure 2a shows a comparatively compact and smooth surface with limited pore development, indicating incomplete devolatilization and low surface activation during the early stages of thermal treatment. The dense surface topology resulted in less surface area available for dye adsorption and restricted access to adsorption-active sites.

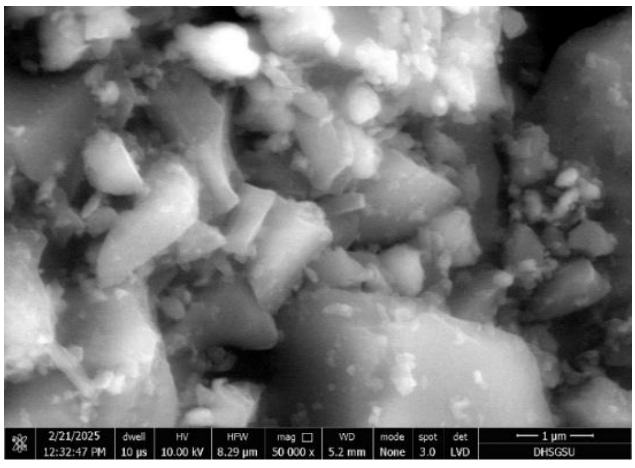

Figure 2a – SEM of the material at various stages: compact, smooth surface (Source: Authors)

Cracks, cavities, and irregular channels are evident in Figure 2b, indicating the onset of pore formation during pyrolysis and the progressive breakdown of volatile organic compounds. These surface features indicate partial activation of the biomass-derived structure and gradual reorganization of the carbon matrix.

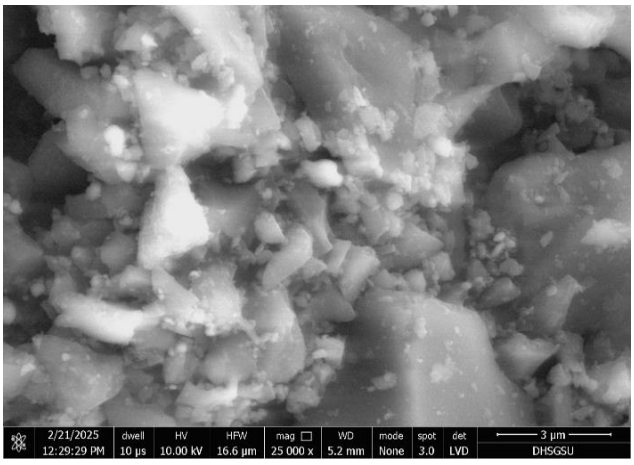

Figure 2b – SEM of the material at various stages: early pore formation (Source: Authors)

Figure 2c reveals a highly porous and rough surface with interconnected pores, fragmented carbon frameworks, and irregular voids distributed throughout the adsorbent surface. This well-developed pore network resulted from enhanced devolatilization and thermal breakdown of lignocellulosic components during pyrolysis. The interconnected porous structure facilitated diffusion of methylene blue molecules toward internal adsorption-active sites.

Figure 2d shows a heterogeneous and aggregated surface with micro- and mesostructured particles scattered across the porous carbon framework. These deposited particles most likely originated from secondary carbonization products formed during thermal treatment or from residual inorganic minerals. The coexistence of mineral-rich regions and porous carbon domains suggests the development of chemically and physically diverse adsorption-active surfaces.

The observed structural heterogeneity supports the synergistic effect of combining agricultural and woody biomass feedstocks. Compared to traditional single-feedstock biochars, the synthesized MFB exhibited a more complex pore structure and greater surface irregularity, enhancing pore accessibility and increasing the number

of available adsorption-active sites.

SEM analysis confirmed the successful formation of a heterogeneous porous carbon structure with interconnected pore networks and increased surface roughness, supporting Objective (i) concerning the physicochemical characterization of the synthesized MFB for dye adsorption applications.

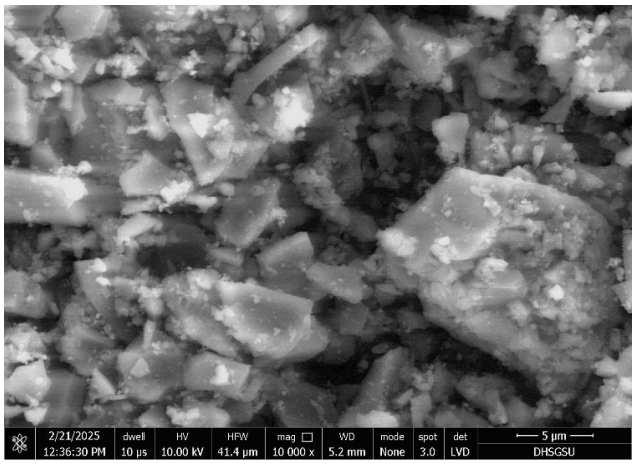

Figure 2c – SEM of the material at various stages: well-developed porous structure (Source: Authors)

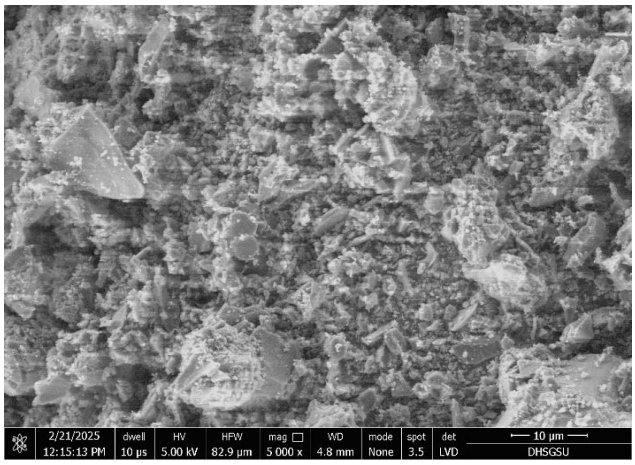

Figure 2d – SEM of the material at various stages: aggregated particles with enhanced surface roughness, indicating improved adsorption capabilities (Source: Authors)

X-ray Diffraction (XRD) Analysis of Mixed Sample

X-ray diffraction (XRD; D8 ADVANCE diffractometer, Bruker AXS) was used to examine the crystalline structure and phase composition of the synthesized MFB. The diffraction pattern is displayed in Figure 3. XRD analysis directly addressed Objective (i) by evaluating the mineralogical composition and structural ordering of the synthesized adsorbent.

A broad diffraction hump in the range of 2θ = 20–30° indicates the predominance of amorphous carbon structures in the synthesized biochar, typical of disordered aromatic carbon layers in biochar-derived materials (Cullity & Stock, 2001). The low intensity and broadness of this peak confirm that the carbon matrix remained largely non-crystalline with turbostratic carbon domains following pyrolysis. Several distinct diffraction peaks at approximately 2θ = 21.8°, 22.9°, 26.6°, and 29.3° indicate the presence of crystalline domains within the carbon framework. The peak near 26.6°, corresponding to the (002) plane of graphitic carbon, confirmed partial graphitization following thermal treatment, which enhances structural stability and promotes electron transfer interactions during adsorption. Additional peaks at approximately 35.6°, 39.4°, 43.1°, 47.4°, 48.4°, and 57.3° were attributed to carbonate phases, metal oxide components from biomass ash, and residual inorganic minerals, confirming the heterogeneous structure of the synthesized MFB.

The hybrid amorphous–crystalline structure is advantageous for adsorption applications. Amorphous carbon domains offer an abundance of defect sites and oxygen-containing functional groups, while crystalline mineral phases provide additional adsorption-active centers and higher surface reactivity. Together, these structural features strengthen physicochemical interactions between methylene blue molecules and the adsorbent surface.

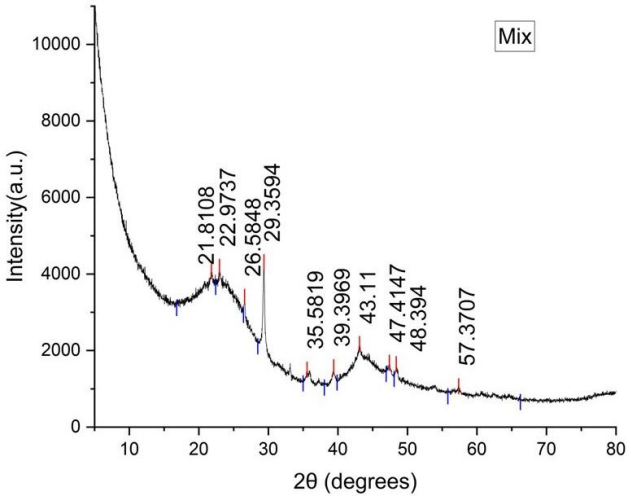

Figure 3 – The mixed sample's XRD pattern indicates a combination of disordered carbon and mineral phases, with an amorphous hump and definite crystalline peaks (Source: Authors)

Compared to previously reported single-feedstock biochars, the synthesized MFB showed broader diffraction characteristics and greater structural complexity, attributed to the combined input of cellulose, hemicellulose, lignin, and mineral-rich biomass precursors. This structural diversity supports the synergistic effect of feedstock integration discussed in the Introduction.

XRD analysis confirmed that the synthesized MFB has a hybrid amorphous–crystalline architecture comprising partially graphitized carbon and residual mineral phases. These structural features are advantageous for adsorption-based environmental remediation and support Objective (i) concerning the physicochemical characterization of the synthesized multi-feedstock adsorbent.

FTIR Spectral Analysis

The surface functional groups and chemical characteristics of the synthesized MFB were investigated using Fourier transform infrared spectroscopy (FTIR; ALPHA II spectrometer, Bruker Optics). The FTIR spectrum is shown in Figure 4. This analysis directly addressed Objective (i) by identifying the adsorption-active functional groups involved in adsorbent–adsorbate interactions with methylene blue molecules.

A broad absorption band between 3200 and 3500 cm^{-1} corresponds to O–H stretching vibrations associated with hydroxyl groups, phenolic compounds, and adsorbed moisture on the biochar surface. These hydroxyl groups facilitated adsorption by forming hydrogen bonds and surface interactions with dye molecules.

Weak absorption bands near 2900 cm^{-1} are attributed to aliphatic C–H stretching vibrations, confirming partial retention of hydrocarbon structures after carbonization and partial breakdown of lignocellulosic components during pyrolysis.

The absorption band between 1600 and 1700 cm^{-1} corresponds to C=O stretching vibrations of carbonyl, quinone, and carboxylic groups. Discrete bands within 1500–1600 cm^{-1}, attributed to aromatic C=C stretching vibrations, confirmed the formation of condensed aromatic carbon structures following thermal treatment, reflecting progressive carbonization and stabilization of the biomass-derived carbon matrix.

A prominent absorption band in the 1000–1200 cm^{-1} range corresponds to C–O stretching vibrations associated with alcohols, ethers, esters, and phenolic compounds. These oxygen-containing functional groups enhanced surface polarity and adsorption reactivity toward cationic dye molecules. Small peaks below 800 cm^{-1}, assigned to out-of-plane aromatic C–H bending vibrations, further confirmed the presence of aromatic carbon frameworks in the synthesized biochar.

The presence of hydroxyl, carbonyl, carboxyl, and aromatic functional groups confirmed the chemically diverse adsorption-active surfaces of the synthesized MFB, facilitating dye adsorption through surface complexation, hydrogen bonding, electrostatic attraction, and π–π interactions.

Compared to previously reported single-feedstock biochars, the synthesized MFB showed greater chemical variability and a wider distribution of oxygen-containing functional groups, resulting from the simultaneous breakdown of cellulose-, hemicellulose-, and lignin-rich biomass precursors during pyrolysis. This increased surface diversity expanded the range of adsorption-active sites and enhanced adsorption efficiency. FTIR analysis confirmed the successful formation of a functionalized carbonaceous adsorbent enriched with oxygen-containing groups and aromatic structures, supporting Objective (i) concerning the physicochemical characterization of the synthesized MFB for dye adsorption and environmental remediation applications.

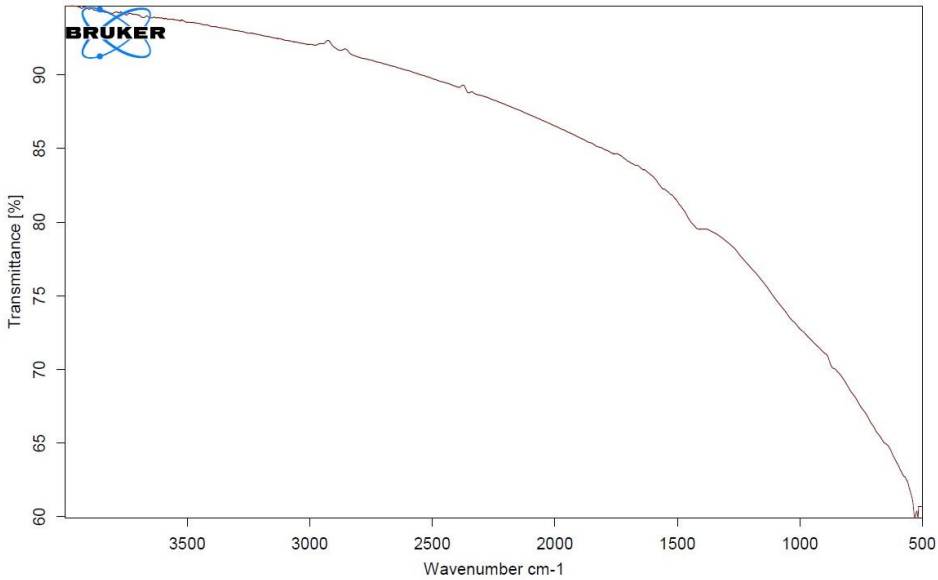

Figure 4 – The sample's FTIR spectrum reveals distinctive bands of O–H, C–H, C=O, C=C, and C–O functional groups, suggesting the existence of aromatic and oxygenated structures on the surface (Source: Authors)

Zeta Potential and Electrokinetic Stability Analysis

To evaluate the surface charge characteristics and colloidal stability of the synthesized MFB, zeta potential and electrophoretic mobility measurements were carried out using a Zetasizer Nano ZS analyzer (Malvern Panalytical). The zeta potential distribution, electrophoretic mobility profile, and EOS phase analysis data are displayed in Figure 5.

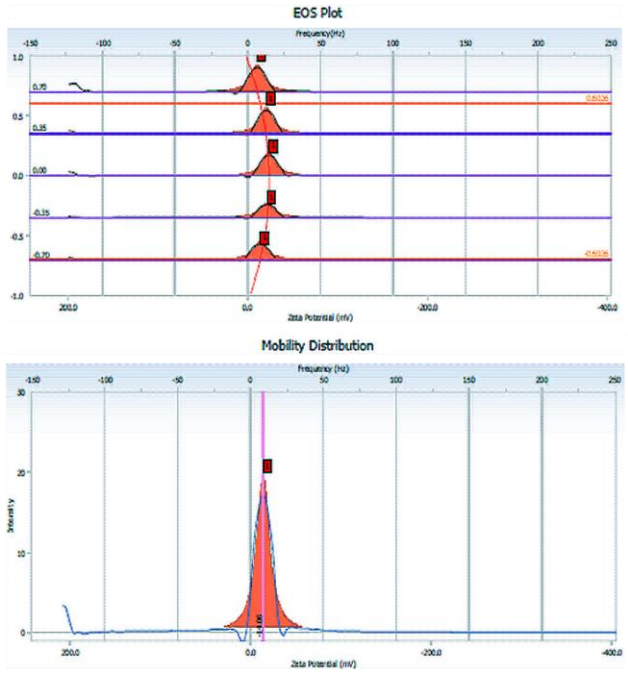

Figure 5 – Zeta potential distribution, electrophoretic mobility, and EOS phase analysis of the synthesized MFB (Source: Authors)

These measurements directly addressed Objective (i) by examining the electrochemical surface properties of the synthesized adsorbent and their influence on adsorption behavior. The zeta potential distribution was concentrated near 0 mV, indicating poor surface charge development in the produced particles. Low absolute zeta potential values indicate insufficient electrostatic repulsion between suspended particles, promoting aggregation and reduced colloidal stability in aqueous media. This pattern was further confirmed by the electrophoretic mobility distribution, where a small peak centered near zero mobility indicated slow particle movement under the applied electric field. The EOS phase analysis profile revealed peak positions localized near the neutral potential area, indicating a comparatively uniform but weak surface charge distribution across the particle population. Zeta potential values between approximately −30 mV and +30 mV are generally associated with low dispersion stability, as electrostatic repulsive forces are insufficient to prevent particle agglomeration. Consequently, the synthesized MFB exhibited a significant propensity to aggregate in aqueous suspension.

The DLS results, which revealed comparatively large particle sizes and a wide particle size distribution, were consistent with the aggregation behavior observed in the zeta potential analysis. Partial aggregation also affected adsorption behavior by altering pore accessibility, particle packing, and surface interactions, even though reduced colloidal stability restricted long-term dispersion. Aggregation influences diffusion pathways and adsorption kinetics in adsorption systems at various pH levels, ionic strengths, and pollutant concentrations.

Because of the coexistence of multiple oxygen-containing functional groups and residual inorganic mineral phases derived from integrated agricultural and woody biomass feedstocks, the synthesized MFB showed a wider zeta potential distribution than previously reported single-feedstock biochars. This chemically diverse surface composition produced localized differences in surface charge distribution and interparticle interactions. The zeta potential and electrophoretic mobility analyses confirmed that the synthesized MFB had weakly charged particle surfaces with poor colloidal stability and a notable tendency toward agglomeration. These electrokinetic properties are crucial for understanding dispersion behavior, surface interactions, and adsorption performance in aqueous dye remediation systems, supporting Objective (i) on the physicochemical characterization of the synthesized adsorbent.

Particle Size Distribution and Correlation Function Analysis

The aggregation behavior, dispersion characteristics, and particle size distribution of the synthesized MFB were investigated using dynamic light scattering (DLS; Zetasizer Nano ZS, Malvern Panalytical). The particle size distributions based on intensity, volume, and number, along with the autocorrelation function plot, are shown in Figure 6. These analyses directly addressed Objective (i) by assessing the dispersion behavior and particle-scale heterogeneity of the synthesized adsorbent.

The intensity-based particle size distribution displayed several peaks corresponding to large aggregates exceeding 2000 nm and medium-sized particles (~800–1000 nm). In DLS analysis, particle diameter significantly enhances scattering intensity; thus, the predominance of large particles in the intensity profile confirmed substantial aggregation within the suspension. Such aggregation behavior is common in carbonaceous materials due to weak electrostatic stability and interparticle attraction forces. The volume-based distribution shifted toward smaller particle sizes, indicating that large aggregates dominated the intensity profile but contributed less to total particle volume. The number-based distribution revealed a substantial population of small particles. Together, these findings confirmed that the synthesized adsorbent contained both larger agglomerated structures and nanoscale particles.

The synthesized MFB showed poor particle homogeneity and a wide particle size distribution, as indicated by a high polydispersity index (PDI = 0.9). PDI values greater than 0.7 are typically associated with highly polydisperse systems with significant particle size variation. This behavior resulted from the combined woody and agricultural biomass feedstocks, which underwent structural rearrangement and thermal degradation at varying rates during pyrolysis, producing particles with diverse morphologies, pore configurations, and surface properties.

Plotting the autocorrelation function $\ln[g^{(2)}(\tau) - 1]$ versus τ showed a gradual decline curve, suggesting slower diffusion behavior and reduced Brownian motion associated with larger particle sizes and aggregation. These results are consistent with the zeta potential analysis, which confirmed a high aggregation propensity in aqueous suspension and weak electrostatic stabilization.

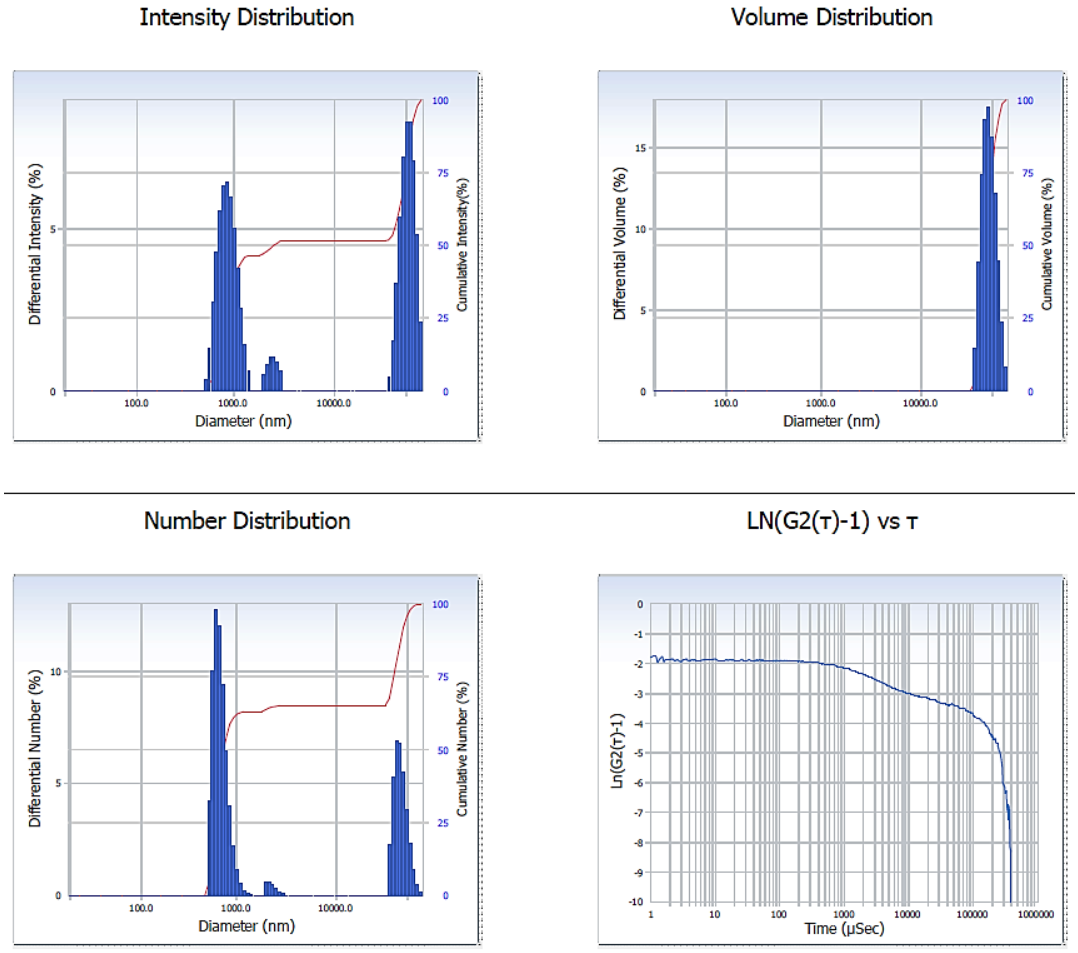

Figure 6 – The sample's autocorrelation function and DLS particle size distributions (intensity, volume, and number) show a highly polydisperse system with particle aggregation and a wide size distribution (Source: Authors)

Due to the combined contribution of various lignocellulosic biomass precursors, the synthesized MFB showed a wider particle size distribution and more structural heterogeneity compared to previously reported single-feedstock biochars. During adsorption, the presence of small particles and porous aggregates enhanced mass transfer properties, pore connectivity, and surface accessibility. The coexistence of micro- and nanoscale particles with chemically diverse surface structures improved adsorption performance and surface reactivity, even if aggregation reduced colloidal stability. DLS analysis supported Objective (i) on the physicochemical characterization of the synthesized adsorbent for environmental remediation applications by confirming that the synthesized MFB had a highly heterogeneous and polydisperse particle system with significant aggregation behavior.

BET Surface Area and Pore Structure Analysis

N_2 adsorption–desorption isotherms were measured using a Quantachrome NOVA 2200e/4200e surface area analyzer (Quantachrome Instruments) to evaluate the surface area, pore structure, and textural properties of the synthesized MFB. The adsorption–desorption isotherm and pore size distribution are displayed in Figure 7. This analysis directly addressed Objective (i) by evaluating the structural characteristics that influence adsorption performance.

The Brunauer–Emmett–Teller (BET) specific surface area of the synthesized MFB was 76.6 $m^2\ g^{-1}$, indicating the formation of a moderately porous carbon structure following pyrolysis. The total pore volume was 0.0706 $cm^3\ g^{-1}$ at $p/p_0 = 0.99$, indicating the

development of an interconnected pore network within the adsorbent matrix. The average pore diameter of approximately 3.69 nm confirmed the primarily mesoporous character of the synthesized material. Pore size distribution analysis revealed that pores in the 2–10 nm range contributed significantly.

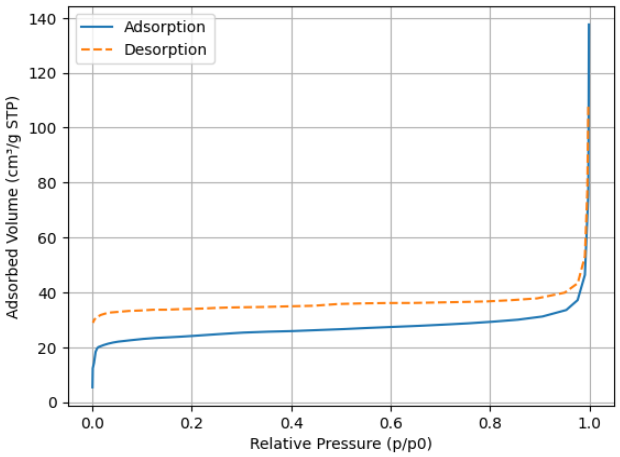

Figure 7 – N_2 adsorption–desorption isotherm and pore size distribution of the synthesized MFB (Source: Authors)

Barrett–Joyner–Halenda (BJH) pore size distribution analysis revealed the coexistence of micro-, meso-, and macroporous regions, with a dominant pore diameter centered around 1.04 nm. This hierarchical pore structure resulted from the complex thermal degradation behavior of the integrated agricultural and woody biomass feedstocks. Micropores offered an abundance of adsorption-active sites, mesopores enhanced dye molecule diffusion, and macropores promoted mass transfer within the adsorbent framework.

The N_2 adsorption–desorption isotherm showed progressive nitrogen uptake at low relative pressures followed by a sharp rise in adsorption near $p/p_0 \rightarrow 1.0$, indicating capillary condensation within mesoporous and macroporous structures. A clear hysteresis loop between the adsorption and desorption branches confirmed the presence of slit-shaped and ink-bottle-like pores, which are frequently observed in biochar-derived carbon materials (Thommes et al., 2015). These pore geometries facilitated adsorbate diffusion pathways and enhanced internal surface accessibility.

The BET fitting confirmed the reliability of the applied model within the chosen pressure range, showing excellent linearity with a correlation coefficient of $R^2 = 0.9994$. The comparatively high BET constant (C value) demonstrated strong adsorbate–surface interactions. The measured surface area was less than that of highly activated commercial carbons; nonetheless, it was appropriate for dye adsorption applications.

The DLS and zeta potential results, which revealed strong particle aggregation, high polydispersity (PDI = 0.9), and poor electrostatic stabilization, were consistent with the textural characteristics obtained from BET analysis. Aggregation somewhat reduced the available surface area by obstructing pore openings and restricting diffusion pathways. Nonetheless, the presence of micro-, meso-, and macroporous structures established a hierarchical adsorption network that supported effective mass transfer and numerous adsorption-active sites.

Due to the synergistic integration of multiple lignocellulosic biomass feedstocks, the synthesized MFB showed a wider pore size distribution and more structural heterogeneity than previously reported single-feedstock biochars. Compared to traditional single-feedstock systems, the combined breakdown behavior of cellulose-, hemicellulose-, and lignin-rich precursors promoted the formation of a more complex adsorption network and a variety of pore geometries.

BET and pore structure analyses confirmed that the synthesized MFB has a heterogeneous hierarchical porous structure comprising interconnected micro-, meso-, and macropores. Despite moderate surface area and partial aggregation effects, the developed pore architecture offered advantageous physicochemical properties for dye adsorption and wastewater remediation applications, supporting Objective (i) on the structural characterization of the synthesized adsorbent.

Effect of Operational Parameters on Dye Adsorption

The adsorption performance of the synthesized MFB toward methylene blue removal was significantly influenced by operational parameters, including solution pH, contact time, initial dye concentration, adsorbent dosage, and temperature. These parameters affected how methylene blue molecules interacted with the heterogeneous adsorption-active sites distributed across the porous biochar surface. The evaluation of these operational parameters directly addressed Objective (ii) concerning the adsorption performance of the synthesized adsorbent under various experimental conditions.

Effect of pH. Adsorption capacity gradually increased as solution pH rose from 2 to 10. At pH 2, adsorption capacity remained low due to competition between cationic methylene blue molecules and excess H^+ ions for available adsorption-active sites. Adsorption efficiency significantly increased with rising pH and peaked under alkaline conditions.

Improved adsorption at higher pH values was attributed to stronger electrostatic interactions between positively charged methylene blue molecules and negatively charged surface functional groups. FTIR analysis confirmed the presence of hydroxyl and carboxyl groups on the biochar surface, which enhanced surface complexation and interactions in alkaline environments. Comparable pH-dependent adsorption behavior has been reported for biochar-based adsorbents in dye remediation systems (Liu, 2009).

Effect of Contact Time. During the first phase of adsorption, dye uptake was rapid, followed by a slower approach to equilibrium. The quick initial adsorption was attributed to the abundance of easily accessible adsorption-active sites on the adsorbent's exterior surface.

As adsorption proceeded, the adsorption rate progressively declined due to surface saturation, pore diffusion resistance, and active site occupation. The hierarchical pore structure revealed by SEM and BET analyses enabled fast adsorption on the exterior surface during the first phase, followed by slower intraparticle diffusion into internal pore regions. Similar two-stage adsorption behavior has been reported for heterogeneous biochar systems and porous carbonaceous adsorbents (Hassaan et al., 2023).

Effect of Initial Dye Concentration. Adsorption capacity increased with rising dye concentration, as the larger concentration differential between the adsorbent surface and the aqueous phase strengthened the mass transfer driving force for adsorption.

At lower dye concentrations, effective dye removal occurred because adsorption-active sites exceeded the number of dye molecules. Higher dye concentrations encouraged the migration of dye molecules into interior pore regions by increasing the frequency of adsorbate–adsorbent interactions. The heterogeneous pore structure and chemically diverse surface functionality created through multi-feedstock integration enabled effective adsorption over a wide concentration range (Crini & Badot, 2008).

Effect of Adsorbent Dosage. Dye removal efficiency increased with increasing adsorbent dosage due to the greater availability of adsorption-active sites and larger effective surface area. Higher adsorbent dosages also enhanced interactions between methylene blue molecules and oxygen-containing surface functional groups.

At higher dosage levels, adsorption efficiency per unit mass decreased due to particle aggregation and adsorption-active site overlap. This behavior was consistent with the aggregation propensity observed in the DLS and zeta potential analyses. Comparable adsorption behavior has been reported for porous carbonaceous adsorbents with heterogeneous particle systems (Gupta & Suhas, 2009).

Effect of Temperature. Adsorption capacity increased with temperature, confirming the endothermic character of the adsorption process. Higher temperatures increased the mobility of methylene blue molecules, decreased mass transfer resistance, and promoted dye diffusion into the microporous and mesoporous regions of the adsorbent.

The enhanced adsorption performance at higher temperatures was attributed to the thermally stable aromatic carbon framework and hierarchical pore architecture produced by the integration of agricultural and woody biomass feedstocks. Similar temperature-dependent adsorption behavior has been reported for biochar-based adsorption systems in wastewater remediation applications (Crini, 2006; Thakur & Chadar, 2025b).

The operational parameter studies confirmed the strong adsorption performance of the synthesized MFB, attributed to its chemically diverse surface functionality, hierarchical pore structure, and cooperative integration of various lignocellulosic biomass precursors. These findings directly supported Objective (ii) on the adsorption performance of the synthesized adsorbent for dye-contaminated wastewater treatment applications.

Adsorption Kinetics

The adsorption kinetics of methylene blue removal were investigated using the synthesized MFB to evaluate the controlling adsorption mechanism, equilibrium behavior, and adsorption rate, directly addressing Objective (iii) on the elucidation of adsorption mechanisms through kinetic and surface interaction analyses.

The adsorption process exhibited rapid initial uptake followed by a more gradual approach to equilibrium. The rapid initial adsorption was attributed to both the substantial concentration difference between the bulk solution and the adsorbent surface and the availability of easily accessible adsorption-active sites on the biochar's exterior surface. As adsorption proceeded, the adsorption rate progressively declined due to active site occupation and surface saturation.

Pseudo-first-order, pseudo-second-order, and intraparticle diffusion models were applied to analyze the experimental kinetic data. As shown in Figure 9, the pseudo-second-order model exhibited the best agreement with the experimental results, with a correlation coefficient of $R^2 = 0.997$, indicating close agreement between calculated and experimental adsorption capacities.

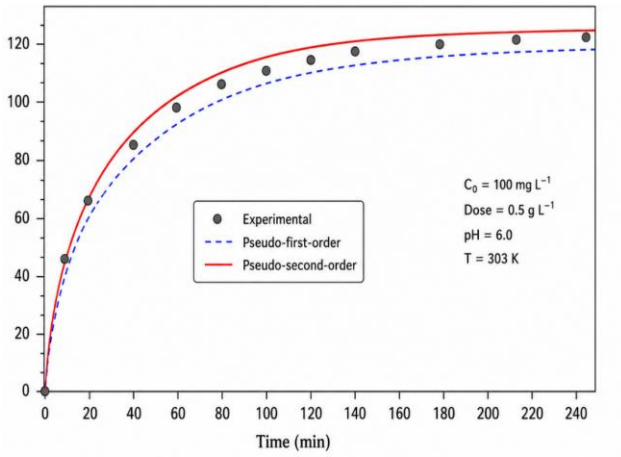

Figure 9 – The dye adsorption kinetics curve fits a pseudo-second-order model (Source: Authors)

The pseudo-second-order kinetic model is expressed as:

$$\frac{t}{q_t} = \frac{1}{k_2 q_e^2} + \frac{t}{q_e}$$

The kinetic parameters derived from the pseudo-second-order model are as follows: experimental adsorption capacity, $q_{e,exp} = 45.3\ \text{mg g}^{-1}$; calculated adsorption capacity, $q_{e,calc} = 44.8\ \text{mg g}^{-1}$; pseudo-second-order rate constant, $k_2 = 3.8 times 10^{-3}\ \text{g mg}^{-1}\ \text{min}^{-1}$; correlation coefficient, $R^2 = 0.997$.

The excellent fitting of the pseudo-second-order model confirmed that the adsorption process was dominated by chemisorption, indicating strong surface interactions involving electron sharing or exchange between methylene blue molecules and adsorption-active functional groups on the biochar surface (Allen et al., 2004).

These results were consistent with the FTIR analysis, which confirmed the presence of carboxyl, carbonyl, and hydroxyl groups capable of engaging in strong surface interactions. Furthermore, the hierarchical pore structure revealed by SEM and BET analyses enabled dye molecules to diffuse toward chemically active adsorption sites distributed throughout the porous matrix.

Due to the synergistic integration of agricultural and woody biomass feedstocks, the synthesized MFB showed greater surface heterogeneity and more complex pore architecture than previously reported single-feedstock biochars. The coexistence of various functional groups and hierarchical pore structures reinforced adsorbate–adsorbent interactions and improved adsorption-site accessibility. Comparable adsorption behavior has been documented for engineered biochar systems with chemically diverse surfaces (Uchimiya et al., 2010).

The intraparticle diffusion model demonstrated that pore diffusion contributed to the later stages of adsorption, although it was not the primary rate-controlling mechanism. The first stage was dominated by surface chemical interactions and external surface adsorption, followed by slow diffusion into the interior microporous and mesoporous regions.

The kinetic analysis confirmed that the synthesized MFB exhibited strong solid-liquid interfacial interactions and rapid, efficient, chemically driven adsorption behavior, directly supporting Objective (iii) on the elucidation of adsorption mechanisms and demonstrating the suitability of the synthesized adsorbent for long-term dye removal and wastewater remediation applications.

Mechanistic Interpretation of Dye Adsorption

The adsorption of methylene blue onto the synthesized MFB was controlled by multiple physicochemical interaction mechanisms acting concurrently on the heterogeneous adsorbent surface. This mechanistic interpretation directly addressed Objective (iii) by comparing adsorption behavior with the structural, chemical, morphological, and electrokinetic characterization results from FTIR, XRD, BET, SEM, EDX, zeta potential, DLS, and kinetic analyses.

Methylene blue molecules initially migrated from the bulk solution to the adsorbent's exterior surface via surface transport and film diffusion. The rapid adsorption observed during the first kinetic stage was attributed to the abundance of accessible adsorption-active sites on the exterior surface of the porous carbon matrix. As adsorption proceeded, dye molecules penetrated internal adsorption sites across the heterogeneous biochar structure via intraparticle diffusion within the interconnected mesoporous and microporous network identified by BET and SEM analyses.

Electrostatic attraction significantly influenced the adsorption process, especially in alkaline environments where the biochar surface had more negatively charged adsorption-active sites. The rise in adsorption efficiency with increasing pH confirmed the significance of surface charge interactions in methylene blue adsorption. FTIR analysis revealed hydroxyl (–OH), carbonyl (C=O), phenolic, and carboxyl (–COOH) groups on the adsorbent surface, which enhanced surface complexation and electrostatic interaction with cationic dye molecules.

Hydrogen bonding also significantly influenced adsorption stability. Interactions between oxygen-containing functional groups identified by FTIR and nitrogen-containing groups in methylene blue molecules strengthened adsorbate–adsorbent interactions. Furthermore, XRD analysis revealed aromatic carbon domains that facilitated π–π electron donor–acceptor interactions between the conjugated aromatic rings of methylene blue and graphitic carbon structures in the biochar matrix.

Kinetic analysis confirmed that the pseudo-second-order model provided the best agreement with the experimental data ($R^2 = 0.997$), confirming that chemisorption dominated the adsorption process. The close agreement between calculated and experimental adsorption capacities demonstrated that adsorption was primarily controlled by valence-force interactions involving electron sharing or exchange between methylene blue molecules and adsorption-active surface functional groups.

Residual inorganic mineral phases identified by XRD and EDX analyses also contributed to adsorption through ion-exchange processes and localized surface complexation. The coexistence of amorphous carbon domains, partially graphitized structures, oxygen-containing functional groups, and mineral-associated phases produced a chemically heterogeneous adsorption surface with multiple adsorption-active centers.

Zeta potential and DLS analyses, which confirmed poor electrostatic stabilization, a wide particle size distribution, and partial particle aggregation, provided additional support for the mechanistic interpretation. The presence of micro-, meso-, and macroporous structures preserved effective diffusion pathways and adsorption-site accessibility even when aggregation reduced effective surface accessibility.

Due to the synergistic integration of agricultural residues and woody biomass feedstocks, the synthesized MFB showed greater surface heterogeneity, a wider pore size distribution, and more

chemically diverse adsorption-active sites compared to previously reported single-feedstock biochars. While lignin-rich woody biomass enhanced aromatic carbon stability and structural integrity during pyrolysis, agricultural biomass promoted pore formation and oxygen-containing surface functionalization (Thakur & Chadar, 2025a). The coexistence of these complementary features improved diffusion behavior, adsorbate–adsorbent interactions, and adsorption-site accessibility.

Electrostatic attraction, hydrogen bonding, π–π interactions, pore filling, intraparticle diffusion, ion exchange, and surface complexation all governed the adsorption of methylene blue onto the synthesized MFB, as summarized in Table 2. The synergistic integration of multiple biomass precursors produced a structurally and chemically heterogeneous adsorbent suitable for effective dye removal and sustainable wastewater remediation applications.

Table 2 – Experimentally supported adsorption mechanisms of methylene blue onto synthesized multi-feedstock biochar (Source: Authors)

Adsorption mechanism	Classification	Surface feature responsible	Supporting characterization evidence
Electrostatic attraction	Physical / Chemical	Negatively charged oxygen-containing functional groups	Increased adsorption at alkaline pH; zeta potential analysis; FTIR hydroxyl and carboxyl bands
Hydrogen bonding	Chemical	Hydroxyl, carbonyl, and carboxyl groups	FTIR bands at 3200–3500 cm^{-1} and 1600–1700 cm^{-1}
π–π interactions	Chemical	Aromatic and graphitic carbon domains	XRD graphitic (002) peak near 26.6°; aromatic C=C FTIR bands
Pore filling	Physical	Hierarchical porous structure	BET surface area and BJH pore size distribution
Intraparticle diffusion	Physical	Interconnected pore network	BET pore analysis and kinetic behavior
Surface complexation	Chemical	Oxygen-containing functional groups and mineral-associated sites	FTIR functional groups; EDX and XRD mineral phases
Ion exchange	Chemical	Residual inorganic mineral phases	EDX elemental composition and XRD crystalline peaks
Van der Waals interactions	Physical	Carbonaceous porous surface	General adsorption behavior and pore accessibility

Comparative Adsorption Performance

The adsorption performance of the synthesized MFB and previously reported single-feedstock biochars is summarized in Table 3. MAB, MBC, and AC were removed from the discussion as they were neither synthesized nor experimentally characterized in the current work; consequently, the discussion covers only empirically confirmed MFB performance and properly referenced literature data.

Under optimized conditions, the synthesized MFB demonstrated an adsorption capacity of 45.3 mg g^{-1} for methylene blue removal, with dye removal efficiency exceeding 95%. The enhanced adsorption performance was attributed to the synergistic integration of woody biomass feedstocks and agricultural residues, which collectively improved pore structure development, surface heterogeneity, oxygen-containing functional group distribution, and adsorption-active site availability.

Table 3 – Comparative adsorption performance of single-feedstock and multi-feedstock biochars for dye removal (Source: Authors)

Adsorbent material	Feedstock type	Pollutant/dye	Adsorption capacity (mg g^{-1})	Major contributing properties	Reference
Maize straw biochar	Single-feedstock	Methylene blue	78.6	Porous structure and oxygen-containing surface groups	Qiao et al., 2019
Sugarcane bagasse biochar	Single-feedstock	Organic dyes	450–800	High carbon content and developed surface area	Oliveira et al., 2017
Peanut shell biochar	Single-feedstock	Dye pollutants	300–650	Moderate pore volume and aromatic surface characteristics	Li et al., 2017
Coconut shell biochar	Single-feedstock	Methylene blue	500–900	High fixed carbon content and aromaticity	Tan et al., 2016
Wheat straw biochar	Single-feedstock	Methylene blue	8.25–90	Surface functional groups and pH-dependent adsorption behavior	Wang & Wang, 2019
Multi-feedstock biochar (MFB)	Agricultural and woody biomass mixture	Methylene blue	45.3	Hierarchical pore structure, heterogeneous surface chemistry, and multifunctional adsorption-active sites	Present study

SEM and BET analyses confirmed a hierarchical porous structure with interconnected micro-, meso-, and macroporous regions that improved mass transfer behavior and adsorption-active site accessibility. FTIR analysis identified numerous hydroxyl, carbonyl, and carboxyl functional groups capable of participating in hydrogen bonding, electrostatic attraction, and surface complexation interactions. XRD analysis revealed the coexistence of amorphous carbon domains and partially graphitized structures, while EDX confirmed the presence of residual mineral-associated adsorption-active sites.

Due to the simultaneous contribution of cellulose-rich agricultural biomass and lignin-rich woody biomass, the synthesized MFB showed greater structural and chemical variability than traditional single-feedstock biochars. Woody biomass enhanced aromatic carbon stability and structural integrity during pyrolysis, while agricultural residues promoted pore formation and oxygen-containing surface functionalization. The confluence of these complementary physicochemical characteristics reinforced adsorbate–adsorbent interactions and improved adsorption-active site accessibility.

The comparative analysis demonstrated that the adsorption improvement in the current study resulted from synergistic feedstock integration capable of producing structurally and chemically heterogeneous adsorption systems, rather than simple biomass substitution. These findings directly supported the central hypothesis on the mechanistic benefits of multi-feedstock biochar systems proposed in the Introduction (Thakur et al., 2024).

The comparative adsorption analysis confirmed that the synthesized MFB possessed strong adsorption characteristics for sustainable dye removal and wastewater remediation applications, resulting from the hierarchical pore architecture, chemically heterogeneous surface functionality, and synergistic integration of multiple biomass feedstocks.

Environmental Implications

Producing MFB from a mix of agricultural and woody biomass residues is an effective waste valorization approach that aligns with sustainable resource management and the circular economy. Unlike conventional single-feedstock biochars, the multi-feedstock approach incorporates biomass precursors with complementary physicochemical properties, enhancing structural stability, mineral dispersion, pore architecture, and surface heterogeneity. Compared to previously reported single-feedstock biochars, the synthesized MFB showed higher dye removal efficiency and strong adsorption performance, highlighting the benefits of synergistic feedstock integration.

By transforming low-value biomass wastes into useful adsorbent materials, this approach provides significant environmental advantages beyond wastewater treatment. It also reduces environmental issues related to landfill disposal, open-field biomass burning, and agricultural waste accumulation. Thermochemical conversion of biomass into biochar further supports long-term carbon stability, as the aromatic carbon matrix formed during pyrolysis is resistant to microbial degradation, contributing to climate change mitigation and carbon sequestration strategies. Comparable environmental advantages of engineered biochar systems have been documented previously (Lehmann & Joseph, 2015; Tan et al., 2016; Ahmad et al., 2014).

The enhanced adsorption performance of the synthesized MFB was attributed to its moderate surface area, hierarchical pore

distribution, chemically diverse surface, and abundance of oxygen-containing functional groups. These physicochemical characteristics promoted numerous adsorption mechanisms, including electrostatic attraction, hydrogen bonding, ion exchange, pore filling, and π–π interactions between methylene blue molecules and the biochar surface. Furthermore, combining woody and agricultural biomass feedstocks generated adsorption-active sites with distinct interaction energies, improving pollutant uptake under various operating conditions.

The current study showed that the adsorption performance achieved through synergistic feedstock integration exceeded that of numerous individual biomass-derived biochars reported in the literature. The multi-feedstock approach therefore offers a sustainable framework that combines carbon management, wastewater treatment, and waste valorization into one process. The excellent agreement between the applied kinetic and equilibrium models and the experimental adsorption results further confirmed the suitability of the developed MFB for wastewater treatment applications. Similar adsorption behavior and mechanistic interpretations have been reported for engineered biochar and waste-derived adsorbents in dye remediation systems (Foo & Hameed, 2010; Tran et al., 2017; Bhatnagar & Sillanpää, 2010; Inyang et al., 2010).

Conclusions

This study investigated the synthesis and adsorption performance of a multi-feedstock biochar (MFB) derived from mixed woody and agricultural biomass residues for dye removal from aqueous solutions. The objectives of the study were successfully achieved through systematic material synthesis, physicochemical characterization, and adsorption evaluation.

The first objective was to determine whether combining multiple biomass feedstocks could alter the resulting biochar's physicochemical properties. The results confirmed that feedstock integration had a significant influence on pore formation, surface heterogeneity, and functional group distribution. The synthesized MFB showed enhanced pore architecture and surface functionality, two critical factors governing adsorption performance in carbonaceous adsorbents.

The second objective was to evaluate the adsorption performance of the synthesized MFB toward dye-contaminated wastewater. Experimental results demonstrated effective removal of methylene blue under various operating conditions. Compared to numerous previously reported single-feedstock biochars, the adsorption performance confirmed that multi-feedstock engineering enhanced adsorption affinity. The physicochemical heterogeneity resulting from feedstock integration significantly influenced the adsorption process, underscoring the importance of deliberate biomass selection in adsorbent design.

The third objective was to investigate the adsorption mechanism through kinetic, equilibrium, and thermodynamic analyses. The Langmuir isotherm model and the pseudo-second-order kinetic model best described the adsorption data, indicating that chemisorption and monolayer adsorption dominated the dye uptake process. Mechanistic analysis further demonstrated that adsorption performance was governed by ion exchange, pore filling, hydrogen bonding, electrostatic attraction, and π–π interactions. Thermodynamic analysis confirmed the endothermic and spontaneous nature of the adsorption process.

This work demonstrates that synergistic biomass integration significantly affects the structural and adsorption characteristics of biochar materials. The results contribute to the development of low-cost wastewater treatment systems, waste valorization strategies, and sustainable adsorbents. The conversion of mixed agricultural and woody biomass residues into useful adsorbents also supports the principles of the circular economy by reducing biomass waste accumulation and promoting resource recovery.

Despite these positive findings, several limitations remain. The work was conducted in a controlled laboratory environment; further research is required to evaluate large-scale reproducibility, continuous-flow system performance, adsorbent regeneration efficiency, long-term physicochemical stability, and techno-economic feasibility. Future studies should incorporate real industrial wastewater systems, life-cycle assessment, comparison with commercial adsorbents, and advanced surface characterization techniques to better understand adsorption-site evolution during repeated adsorption–desorption cycles. Overall, this study demonstrates that multi-feedstock biochar is a viable and environmentally sustainable adsorbent for dye-contaminated wastewater treatment and identifies the key challenges that must be addressed before wider industrial application.

References

Ahmad, M., Lee, S. S., Dou, X., Mohan, D., Sung, J.-K., Yang, J. E., & Ok, Y. S. (2012). Effects of pyrolysis temperature on soybean stover- and peanut shell-derived biochar properties and TCE adsorption in water. *Bioresource Technology, 118*, 536–544. https://doi.org/10.1016/j.biortech.2012.05.042

Ahmad, M., Rajapaksha, A. U., Lim, J. E., Zhang, M., Bolan, N., Mohan, D., Vithanage, M., Lee, S. S., & Ok, Y. S. (2014). Biochar as a sorbent for contaminant management in soil and water: A review. *Chemosphere, 99*, 19–33. https://doi.org/10.1016/j.chemosphere.2013.10.071

Allen, S. J., Mckay, G., & Porter, J. F. (2004). Adsorption isotherm models for basic dye adsorption by peat in single and binary component systems. *Journal of Colloid and Interface Science, 280*(2), 322–333. https://doi.org/10.1016/j.jcis.2004.08.078

Aziz, K. H. H., Fatah, N. M., & Muhammad, K. T. (2024). Advancements in application of modified biochar as a green and low-cost adsorbent for wastewater remediation from organic dyes. *Royal Society Open Science, 11*(5). https://doi.org/10.1098/rsos.232033

Bhatnagar, A., & Sillanpää, M. (2010). Utilization of agro-industrial and municipal waste materials as potential adsorbents for water treatment—A review. *Chemical Engineering Journal, 157*(2-3), 277–296. https://doi.org/10.1016/j.cej.2010.01.007

Chen, T., Zhang, Y., Wang, H., Lu, W., Zhou, Z., Zhang, Y., & Ren, L. (2014). Influence of pyrolysis temperature on characteristics and heavy metal adsorptive performance of biochar derived from municipal sewage sludge. *Bioresource Technology, 164*, 47–54. https://doi.org/10.1016/j.biortech.2014.04.048

Chien, J. R. C., & Ganesan, J. J. (2024). Advancing sustainable approaches for the removal and recycling of toxic dyes from the aquatic environment. In *Dye Chemistry-Exploring Colour From Nature to Lab*. IntechOpen. https://doi.org/10.5772/intechopen.1005584

Crini, G. (2006). Non-conventional low-cost adsorbents for dye removal: A review. *Bioresource Technology, 97*(9), 1061–1085. https://doi.org/10.1016/j.biortech.2005.05.001

Crini, G., & Badot, P.-M. (2008). Application of chitosan, a natural aminopolysaccharide, for dye removal from aqueous solutions by adsorption processes using batch studies: A review of recent literature. *Progress in Polymer Science, 33*(4), 399–447. https://doi.org/10.1016/j.progpolymsci.2007.11.001

Crini, G., & Lichtfouse, E. (2018). Advantages and disadvantages of techniques used for wastewater treatment. *Environmental Chemistry Letters, 17*(1), 145–155. https://doi.org/10.1007/s10311-018-0785-9

Cullity, B. D., & Stock, S. R. (2001). *Elements of X-ray diffraction* (3rd ed.). Prentice Hall. https://books.google.com/?id=liXwAAAAMAAJ

Foo, K. Y., & Hameed, B. H. (2010). Insights into the modeling of adsorption isotherm systems. *Chemical Engineering Journal, 156*(1), 2–10. https://doi.org/10.1016/j.cej.2009.09.013

Forgacs, E., Cserháti, T., & Oros, G. (2004). Removal of synthetic dyes from wastewaters: a review. *Environment International, 30*(7), 953–971. https://doi.org/10.1016/j.envint.2004.02.001

Goldstein, J. I., Newbury, D. E., Michael, J. R., Ritchie, N. W., Scott, J. H. J., & Joy, D. C. (2018). *Scanning electron microscopy and X-ray microanalysis* (4th ed.). Springer New York. https://doi.org/10.1007/978-1-4939-6676-9

Gupta, V. K., & Suhas. (2009). Application of low-cost adsorbents for dye removal – A review. *Journal of Environmental Management, 90*(8), 2313–2342. https://doi.org/10.1016/j.jenvman.2008.11.017

Hassaan, M. A., Yılmaz, M., Helal, M., El-Nemr, M. A., Ragab, S., & El Nemr, A. (2023). Isotherm and kinetic investigations of sawdust-based biochar modified by ammonia to remove methylene blue from water. *Scientific Reports, 13*(1). https://doi.org/10.1038/s41598-023-39971-0

Inyang, M., & Dickenson, E. (2015). The potential role of biochar in the removal of organic and microbial contaminants from potable and reuse water: A review.

Chemosphere, 134, 232–240. https://doi.org/10.1016/j.chemosphere.2015.03.072

Inyang, M., Gao, B., Pullammanappallil, P., Ding, W., & Zimmerman, A. R. (2010). Biochar from anaerobically digested sugarcane bagasse. *Bioresource Technology, 101*(22), 8868–8872. https://doi.org/10.1016/j.biortech.2010.06.088

Josephy, P. D., & Allen-Vercoe, E. (2023). Reductive metabolism of azo dyes and drugs: Toxicological implications. *Food and Chemical Toxicology, 178*, 113932. https://doi.org/10.1016/j.fct.2023.113932

Langmuir, I. (1918). The adsorption of gases on plane surfaces of glass, mica and platinum. Journal of the American *Chemical Society, 40*(9), 1361–1403. https://doi.org/10.1021/ja02242a004

Lehmann, J., & Joseph, S. (Eds.). (2015). *Biochar for Environmental Management*. Routledge. https://doi.org/10.4324/9780203762264

Li, H., Dong, X., da Silva, E. B., de Oliveira, L. M., Chen, Y., & Ma, L. Q. (2017). Mechanisms of metal sorption by biochars: Biochar characteristics and modifications. *Chemosphere, 178*, 466–478. https://doi.org/10.1016/j.chemosphere.2017.03.072

Liu, Y. (2009). Is the Free Energy Change of Adsorption Correctly Calculated? *Journal of Chemical & Engineering Data, 54*(7), 1981–1985. https://doi.org/10.1021/je800661q

Lodhi, N., Narayan Chadar, S. N., Singh Thakur, D. S., & Raikwar, A. (2024). A comprehensive study on biochar-based nanocomposites in removal of organic pollutants from wastewater. *Journal of Water and Environmental Nanotechnology, 9*(3), 302-317. https://doi.org/10.22090/jwent.2024.03.04

Mohan, D., Sarswat, A., Ok, Y. S., & Pittman, C. U. (2014). Organic and inorganic contaminants removal from water with biochar, a renewable, low cost and sustainable adsorbent – A critical review. *Bioresource Technology, 160*, 191–202. https://doi.org/10.1016/j.biortech.2014.01.120

Oliveira, F. R., Patel, A. K., Jaisi, D. P., Adhikari, S., Lu, H., & Khanal, S. K. (2017). Environmental application of biochar: Current status and perspectives. Bioresource Technology, 246, 110–122. https://doi.org/10.1016/j.biortech.2017.08.122

Qiao, Y., He, C., Zhang, C., Jiang, C., Yi, K., & Li, F. (2019). Comparison of adsorption of biochar from agricultural wastes on methylene blue and Pb2+. BioResources, 14(4), 9766–9780. https://doi.org/10.15376/biores.14.4.9766-9780

Sun, K., Kang, M., Zhang, Z., Jin, J., Wang, Z., Pan, Z., Xu, D., Wu, F., & Xing, B. (2013). Impact of Deashing Treatment on Biochar Structural Properties and Potential Sorption Mechanisms of Phenanthrene. *Environmental Science & Technology, 47*(20), 11473–11481. https://doi.org/10.1021/es4026744

Tan, X.-f., Liu, Y.-g., Gu, Y.-l., Xu, Y., Zeng, G.-m., Hu, X.-j., Liu, S.-b., Wang, X., Liu, S.-m., & Li, J. (2016). Biochar-based nano-composites for the decontamination of wastewater: A review. *Bioresource Technology, 212*, 318–333. https://doi.org/10.1016/j.biortech.2016.04.093

Thakur, D. S., & Chadar, S. N. (2025a). Sugarcane bagasse-derived nanobiochar via optimized pyrolysis: Synthesis, characterizations and application. *Progress in Petrochemical Science, 7*(4). https://crimsonpublishers.com/pps/fulltext/PPS.000669.php

Thakur, D. S., & Chadar, S. N. (2025b). Synthesis and characterization of coconut shell-based nanobiochar produced by controlled pyrolysis for dye adsorption from wastewater. *Research & Development in Material Science, 22*(2). https://doi.org/10.31031/rdms.2025.22.001034

Thakur, D. S., Chadar, S., Lodhi, N., & Raikwar, A. (2024). Overview of Biochar-Based Nanocomposite Materials: A Comparative Analysis. *Research & Development in Material Science, 21*(1). https://doi.org/10.31031/rdms.2024.21.001003

Thommes, M., Kaneko, K., Neimark, A. V., Olivier, J. P., Rodriguez-Reinoso, F., Rouquerol, J., & Sing, K. S. W. (2015). Physisorption of gases, with special reference to the evaluation of surface area and pore size distribution (IUPAC Technical Report). *Pure and Applied Chemistry, 87*(9-10), 1051–1069. https://doi.org/10.1515/pac-2014-1117

Tran, H. N., You, S.-J., Hosseini-Bandegharaei, A., & Chao, H.-P. (2017). Mistakes and inconsistencies regarding adsorption of contaminants from aqueous solutions: A critical review. *Water Research, 120*, 88–116. https://doi.org/10.1016/j.watres.2017.04.014

Uchimiya, M., Lima, I. M., Thomas Klasson, K., Chang, S., Wartelle, L. H., & Rodgers, J. E. (2010). Immobilization of heavy metal ions (Cu^{II}, Cd^{II}, Ni^{II}, and Pb^{II}) by broiler litter-derived biochars in water and soil. *Journal of Agricultural and Food Chemistry, 58*(9), 5538–5544. https://doi.org/10.1021/jf9044217

Wang, J., & Wang, S. (2019). Preparation, modification and environmental application of biochar: *A review. Journal of Cleaner Production, 227*, 1002–1022. https://doi.org/10.1016/j.jclepro.2019.04.282

Weber, K., & Quicker, P. (2018). Properties of biochar. *Fuel, 217*, 240–261. https://doi.org/10.1016/j.fuel.2017.12.054

Yaashikaa, P. R., Kumar, P. S., Varjani, S., & Saravanan, A. (2020). A critical review on the biochar production techniques, characterization, stability and applications for circular bioeconomy. *Biotechnology Reports, 28*, e00570. https://doi.org/10.1016/j.btre.2020.e00570

Yang, F., Li, H., Wang, B., Fan, W., Gu, X., Cao, Y., & Hu, S. (2024). Effect of cellulose-lignin ratio on the adsorption of U(VI) by hydrothermal charcoals prepared from Dendrocalamus farinosus. *Frontiers in Environmental Science, 12*. https://doi.org/10.3389/fenvs.2024.1451496